BRAIN
LETTER TO THE EDITOR

Elevated cholesterol is a common phenotype for dominant and recessive *ATAD3*-associated disorders

Ann-Sophie Kiesel,[1] Lucia Laugwitz,[1,2] Rebecca Buchert,[1] Mona Grimmel,[1] Sarah Baumann,[1] Marc Sturm,[1] Selina Reich,[3,4] Martje G. Pauly,[5] Norbert Brüggemann,[5] Alexander Münchau,[6] Olga Oleksiuk,[7] Matthis Synofzik,[3,4] Tobias B. Haack[1] and Susana Peralta[1]

1 Institute of Medical Genetics and Applied Genomics, University of Tübingen, 72076 Tübingen, Germany
2 Department of Neuropediatrics, Developmental Neurology and Social Pediatrics, University of Tübingen, 72076 Tübingen, Germany
3 Division Translational Genomics of Neurodegenerative Diseases, Hertie Institute for Clinical Brain Research & Center of Neurology, University of Tübingen, 72076 Tübingen, Germany
4 German Center for Neurodegenerative Diseases (DZNE), University of Tübingen, 72076 Tübingen, Germany
5 Department of Neurology/Institute of Neurogenetics, University of Lübeck, 23562 Lübeck, Germany
6 Institute of Systems Motor Science, University of Lübeck, 23562 Lübeck, Germany
7 Hertie Institute for Clinical Brain Research (HIH) and Centre for Integrative Neuroscience (CIN) Imaging Cluster, University of Tübingen, 72076 Tübingen, Germany

Correspondence to: Susana Peralta
Institute of Medical Genetics and Applied Genomics, University of Tübingen, Nägelestraße 5, 72074 Tübingen, Germany
E-mail: susana.peralta-morales@med.uni-tuebingen.de

Correspondence may also be addressed to: Tobias B. Haack
E-mail: tobias.haack@med.uni-tuebingen.de

Recently, Muñoz-Oreja *et al.*[1] reported that elevated cholesterol functions as a compensatory mechanism to increase tolerance to pathological heterozygous dominant-acting *ATAD3A* variants, eventually leading to membrane-embedded cholesterol aggregation in the form of membrane whorls. This excess cholesterol is a cellular and pathological abnormality in *ATAD3*-associated disorder that can cascade to lysosomal insufficiency. Here we present a similar accumulation of free cholesterol and membrane whorls in two unrelated patients' cells carrying pathological bi-allelic *ATAD3A* variants. Our results suggest that increased cholesterol is a common cellular response in both, autosomal dominant and recessive *ATAD3*-associated disorders, supporting the premise reported by Muñoz-Oreja *et al.*[1]

Novel bi-allelic *ATAD3A* variants

We report on four individuals from two different families carrying bi-allelic pathogenic variants in *ATAD3A* (NM_001170535.2) that are associated with a very rare, relatively distinct neurological phenotype (Fig.1A and B). Subjects F1:II.1 and F1:II.2 (siblings from Family 1) were compound heterozygous for a previously reported missense variant in combination with a novel nonsense variant: c.[229C>G]; [1687C>T], p.[(Leu77Val)]; [(p.Gln563*)] (Fig. 1A). The p.Leu77Val variant, which entails the substitution of a conserved leucine (Fig. 1C), has been previously characterized as a mild hypomorphic variant.[2] The novel c.1687C>T, p.Gln563* variant is predicted to introduce a stop codon resulting in a truncated protein (Fig. 1B). Subject F1:II.1 presented with a significant motor development delay, severe dysarthria, dysphagia, horizontal gaze palsy, slowed vertical saccades without the limited range of vertical eye movements, spastic tone elevation of extremities with axial hypotonia, and generalized dystonia. Walking was only possible with support. Her younger sister Subject F1:II.2 had learning difficulties and a diagnosis of attention-deficit/hyperactivity disorder and exhibited a bilateral congenital cataract but no additional neurological impairment. Detailed phenotypic information can be found in the Supplementary material. By exome sequencing, we detected in Subjects F2:II.1 and F2:II.2 (Family 2) the same missense p.Leu77Val variant identified in Family 1 on the maternal allele and a novel splice donor variant on the paternal allele c.384+1G>A, p.? (Fig. 1A and B). Subject F2:II.1 is a 41-year-old female who presented with cognitive impairment and early-onset cerebellar ataxia. Subject F2:II.2 is a male with early onset multisystemic degeneration, characterized by cognitive impairment, pyramidal and mild extrapyramidal symptoms. Additionally, both siblings exhibited bilateral congenital cataracts and chronic progressive external ophthalmoplegia (CPEO).

The identified variants are either absent from public databases such as gnomAD or have a very low allele frequency

Received November 12, 2024. Accepted December 01, 2024. Advance access publication December 12, 2024

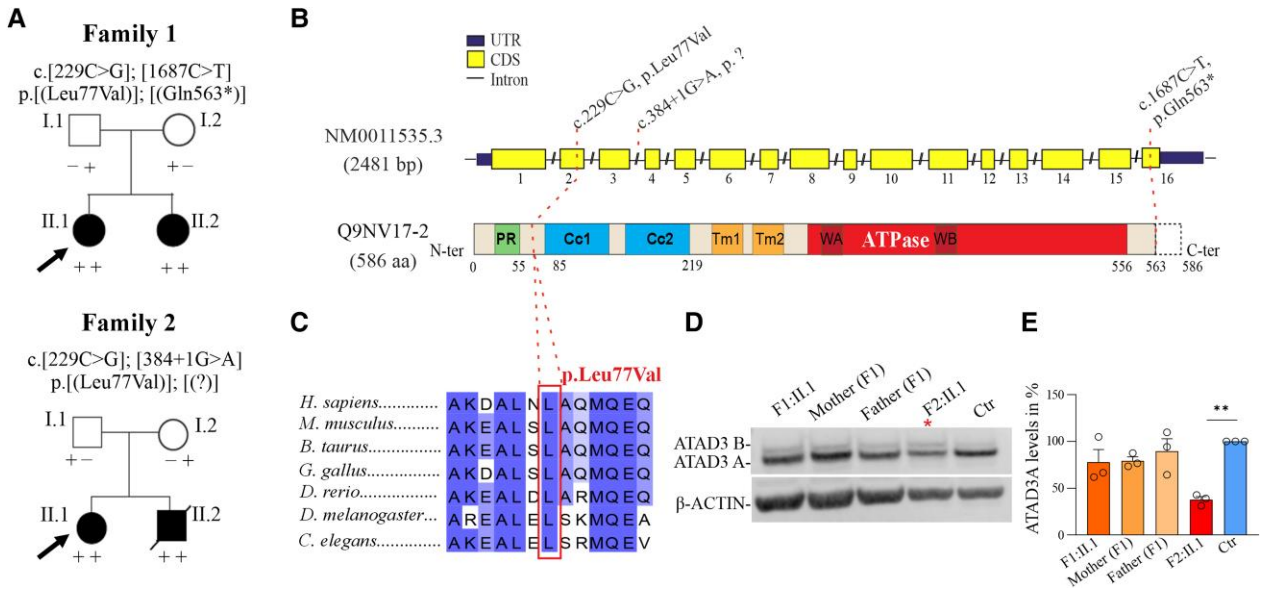

Figure 1 Pedigrees of investigated families with bi-allelic variants in *ATAD3A* and structure of the gene-protein. (**A**) Pedigrees of the investigated subjects with variants in *ATAD3A* (NM_001170535.2). (**B**) Schematic representation of gene structure and protein structure of ATAD3A with predicted domains. Annotations indicate the position of the variants as well as the conservation of the affected amino acid across different species. PR = proline-rich-domain; CC = coiled-coil domain. The transmembrane (TM) domains are shown in orange, the ATPase domain in red, and the Walker A motif and Walker B motifs are denoted with WA and WB, respectively. CDS = coding sequence; UTR = untranslated region. (**C**) Conservation of the affected amino acid (Leu77) across different species. (**D**) Western blot analysis of ATAD3A in whole cell lysates of fibroblast of Subject F1:II.1, her parents, Subject F2:II.1, and control normalized to actin. Immunoblotting with ATAD3 antibody showed two bands, the lower band being compatible with the 66 kDa ATAD3A isoform 2 and the upper faint band being compatible with the 72 kDa ATAD3B protein. (**E**) Quantification of the western blot analysis shown in **D**. The normal data distribution was checked using the Shapiro-Wilk test. Data are organized in a nested table and graphed using a column graph with mean ± standard error of the mean (SEM) ($n = 3$). The values of the patients were analysed with a single sample *t*-test with the reference value 100% resembling the mean of the control. Subject F2:II.1 versus control $^{**}P = 0.003$. Ctr = control.

(Supplementary Table 2), with none of them present in a homozygous state. All variants are predicted to be deleterious by several bioinformatic tools (PolyPhen, Sift, and CADD; Supplementary Table 2).

RNA-sequencing data revealed the presence of both variants in a heterozygous state on the RNA level in Subject F1:II.1 (Supplementary Fig. 1A), which is in line with the general finding that nonsense-mediated decay (NMD) does not take place if a mutation occurs within the last exon. By contrast, in Subject F2:II.1 the RNA transcript predominantly comprises the c.229C>G, p.Leu77Val variant, while transcripts with the c.384+1G>A mutation were mainly subject to degradation via NMD even though there is some evidence of a splice defect leading to skipping of exon 3 in seven reads (Supplementary Fig. 1A). ATAD3A protein levels in Subject F1:II.1 were similar to the levels observed in her parent's fibroblasts (heterozygous carriers) and to the levels exhibited in unrelated control fibroblasts (Fig. 1D and E). This result indicates that the bi-allelic variants c.[229C>G]; [1687C>T], p.[(Leu77Val)];[(Gln563*)] do not affect the stability of the protein. Gln563* is predicted to create a truncated ATAD3A protein, 22 amino acids shorter (around 3 kDa). However, we could not detect a smaller Gln563* variant when the separation of ATAD3A was done on a 7.5% SDS-PAGE. Subject F2:II.1, by contrast, showed reduced ATAD3A levels (43% of the control, Fig. 1D and E), in agreement with the observed halving of *ATAD3A* RNA levels (Supplementary Fig. 1C). Together, our data indicate that c.384+1G>A variant is a null allele.

Bi-allelic ATAD3A mutant cells exhibit increased cholesterol and multilamellar membrane structures

We previously investigated the *in vivo* function of *ATAD3*, using muscle and neuron-specific conditional knockout mouse models.[3,4] This work suggested that loss of *ATAD3* disrupted cristae morphology and altered cholesterol trafficking to the mitochondria in muscle tissue.[3] In addition, perturbed cholesterol metabolism was observed in patients' cells harbouring bi-allelic *ATAD3* gene cluster deletions as well as monoallelic duplications.[5,6] To determine if cholesterol levels were altered in the fibroblasts of our patients with *ATAD3A* bi-allelic variants, we stained free cholesterol with Filipin III (Abcam kit #ab133116), showing significantly more free-cholesterol staining (Fig. 2A and B), with Subject F1:II.1 having nearly four times more and Subject F2:II.1 three times more than controls (Fig. 2B). The observation of increased cholesterol in patients' cells carrying bi-allelic *ATAD3A* variants supports the hypothesis reported by Muñoz-Oreja *et al.*,[1] that elevated cholesterol is a common mechanism to increase the tolerance to pathological *ATAD3A* variants.

We also performed RNA-sequencing of fibroblasts of Subject F1:II.1 in comparison to her healthy parents (heterozygous carriers). We detected a total of 370 differentially expressed genes (DEGs) between the cell lines, of which 232 were up- and 138 downregulated. Interestingly, using the list of identified DEGs, Ingenuity Pathway Analysis revealed that the Superpathway of Cholesterol Biosynthesis, and Cholesterol Biosynthesis I, II and III pathways were among the top five upregulated canonical pathways in the patient's cells (Fig. 2C).

Previous experiments indicated that the p.Leu77Val variant leads to an increase in lysosomal and mito-phagosomal intermediates in *Drosophila* adult muscles.[2] To determine whether we see increased lysosomal content we performed double immunostaining for the lysosomal marker LysoTracker and the mitochondrial dye MitoTracker in the patients' cells. Immunostaining with

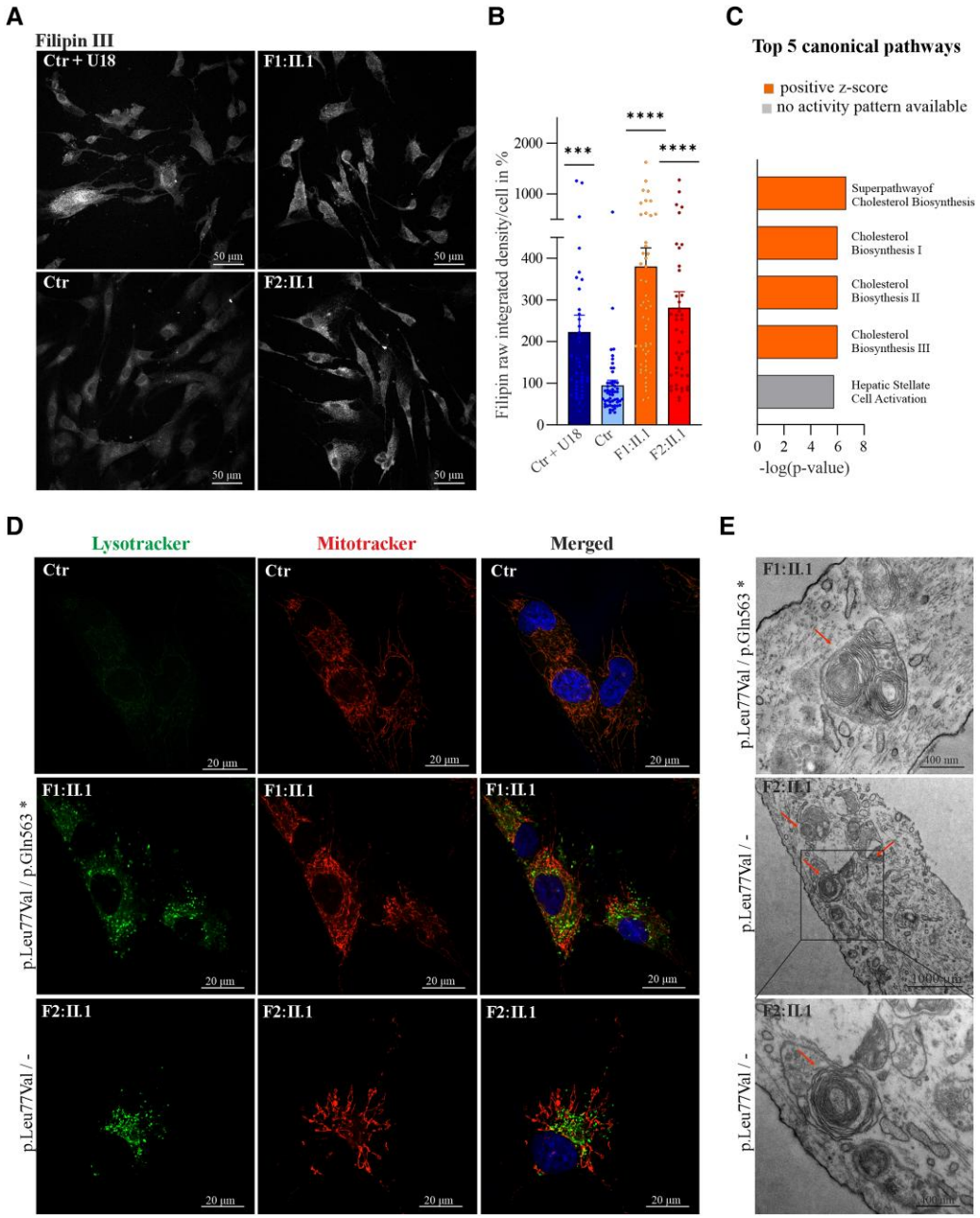

Figure 2 Patient's cells with bi-allelic variants in *ATAD3A* display increased cholesterol levels, increased LysoTracker staining, and structures similar to lamellar bodies. (**A**) Immunofluorescence images of free cholesterol detected by filipin labelling of fibroblasts of Subjects F1:II.1 and F2:II.1, as well as control cell lines. Treatment with 2.5 µM of U18666A for 72 h was used as a positive control. Scale bars = 50 µm. (**B**) Quantification of filipin raw integrated density per cell. Data are shown as per cent of the control (Ctr). Data are the result of three independent experiments for patients and controls and graphed using a column graph representing mean ± standard error of the mean. Then it was analysed with a single sample Wilcoxon test with the reference value 100% resembling the mean of the control. Subject F1:II:1 $P < 0.0001$; F2:II:1 $P = 0.0091$. (**C**) Representation of the five most dysregulated pathways in RNA sequencing-based transcriptome data of Subject F1:II.1's fibroblasts compared to her healthy parents Subjects F1:I.2 and F1:I.1. Analysis was performed on Ingenuity Pathway Analysis (IPA) software (v60467501, QIAGEN). Pathways are sorted in descending order based on their P-values, which are displayed in the graph as –log (P-value). Upregulated pathways are highlighted in orange based on positive z-scores. Pathways with indistinct activation patterns are indicated in grey. (**D**) Confocal images of the fibroblasts of patient and control fibroblasts. The signal of the MitoTracker staining is shown in red, LysoTracker in green and DAPI in blue. Scale bars = 20 µm. (**E**) Transmission electron microscopy images of skin-derived fibroblasts of Subject F1:II.1 and Subject F2:II.1. Arrows indicate structures similar to lamellar bodies contained in lysosomes. Scale bars = 1000 µm (lower magnification); 400 nm (higher magnification).

LysoTracker revealed that the cells carrying bi-allelic variants in *ATAD3A* showed increased activity compared to control cells (Fig. 2D). This is consistent with the observations of Muñoz-Oreja *et al.*[1] that enhanced cholesterol in cells increases the lysosomal content. Transmission electron microscopy (TEM) analysis of patients' cells with *ATAD3A* bi-allelic variants revealed several lysosomes containing multilamellar membrane structures (Fig. 2E, arrows). By contrast, these structures were scarce in the control fibroblasts (Supplementary Fig. 2B). Our results support the findings reported by Muñoz-Oreja *et al.*,[1] that the increased free cholesterol

associated with pathological *ATAD3A* variants accumulates in membrane structures similar to lamellar bodies, and now extend these findings also to bi-allelic *ATAD3A* disease. This cholesterol accumulation in membranes is expected to contribute to the molecular pathomechanism of the disease observed in our patients, given that altered cholesterol trafficking is associated with neurological phenotypes in lysosomal storage disorders such as Niemann-Pick disease type C.[7] Here it might also open new avenues to translational treatment targets geared at restoring cholesterol trafficking.

In addition, we analysed mitochondrial ultrastructure by TEM on patients and control fibroblasts. Patients' cells showed both mitochondria with normal architecture, but also mitochondria with ultrastructural abnormalities, such as the loss of cristae resulting in increased matrix space and/or decreased cristae junctions (Supplementary Fig. 3), not seen in similar quantity in controls. These findings indicate that the bi-allelic variants detected in our patients interfere with mitochondrial cristae shaping or maintenance.

In conclusion, our findings suggest that pathogenic recessive *ATAD3A* variants lead to similar compensatory mechanisms regarding cholesterol metabolism as the dominant variants. However, our fibroblasts show lower intensity of the cellular alterations than previously reported by Muñoz-Oreja *et al.*,[1] indicating a milder response. Our patient's cells carrying bi-allelic variants showed between three and four times more filipin-labelled free cholesterol, while those with dominant mutations exhibited 10 times that of control cells.[1] Further research is needed to understand the similarities and differences in the pathomechanisms of recessive versus dominant *ATAD3A* variants as well as the varying clinical expressivity as observed in our patients. Possibly, the discrepancies in cholesterol aggregation height could be explained by the different molecular defects, as the dominant variants affect a conserved arginine in the ATP domain of ATAD3A, and presumably impair *ATAD3* function by affecting the hydrolysis of the ATP. By contrast, the bi-allelic variants detected in our patients located in the N-terminal (p.Leu77Val), and in the C-terminal (p.Gln563*) domain are predicted to affect the formation of ATAD3A homodimers. Nevertheless, the precise mechanism by which the lack of *ATAD3A* causes a defect in cholesterol trafficking in the mitochondria remains unknown, as its precise function has yet to be determined.

Furthermore, we report two previously unreported variants, p.(Gln563*) and c.(384+1G>A) expanding the list of variants associated with autosomal recessive *ATAD3A* disease. The missense c.229C>G, p.Leu77Val variant was previously detected *in trans* with loss of function alleles in five patients from three unrelated families.[2,8] All those patients exhibited severe neurological phenotypes and deceased before the age of 2 years (Supplementary Table 3). However, our cases from Family 2, carrying the c.229C>G, p.Leu77Val variant, *in trans* with the novel loss of function variant c.(384+1G>A), exhibited a surprisingly mild phenotype, which substantially extend and change the perspective on this variant from previous reports (Supplementary Table 3). Our findings thus underline the wide spectrum of clinical presentations associated with the p.Leu77Val variant, suggesting that other genetic and/or ambient factors influence the onset and severity of the disease making the prognosis of those patients challenging.

Data availability

The authors confirm that the data supporting the findings of this study are available within the article including its Supplementary material. Sanger sequence and RNA-sequencing data are available from the corresponding author, upon reasonable request.

Web resources

CADD, https://cadd.gs.washington.edu/
Ensembl Variant Effect Predictor, https://grch37.ensembl.org/Homo_sapiens/Tools/VEP
GenBank, https://www.ncbi.nlm.nih.gov/genbank/
gnomAD Browser, https://gnomad.broadinstitute.org/
MitoProt II, https://bio.tools/MITOPROT_II
OMIM, https://www.omim.org/
The Human Protein Atlas, http://www.proteinatlas.org/
UCSC (February 2009), https://genome.ucsc.edu

Acknowledgements

We would like to thank Birgit Fehrenbacher and Anneli Vollert (Electron Microscopy Laboratory of the Dermatology Department, University of Tübingen) for their help with the fluorescence and transmission electron microscopy and You-Shan Feng from the Institute for Clinical Epidemiology and Applied Biometrics (IKEAB, University of Tübingen) for her help with the statistical analysis.

Funding

This work was supported by the European Union, project European Rare Disease Research Alliance (ERDERA, # 101156595) (to M.Sy. and T.B.H.); by the German Research Foundation, DFG (BR4328.2-1, GRK1957); by the Michael J Fox Foundation for Parkinson's Research, the Collaborative Center for X-linked Dystonia-Parkinsonism and by the EU Joint Programme Neurodegenerative Disease Research (JPND).

Competing interests

M.Sy. has received consultancy honoraria from Ionis, UCB, Prevail, Orphazyme, Biogen, Servier, Reata, GenOrph, AviadoBio, Biohaven, Zevra, Lilly, and Solaxa, all unrelated to the present manuscript. Norbert Brüggemann has received honaria from Abbott, Abbvie, Biogen, Biomarin, Bridgebio, Centogene, Esteve, Ipsen, Merz, Teva, Zambon.

Supplementary material

Supplementary material is available at *Brain* online.

References

1. Muñoz-Oreja M, Sandoval A, Bruland O, et al. Elevated cholesterol in ATAD3 mutants is a compensatory mechanism that leads to membrane cholesterol aggregation. *Brain*. 2024;147:1899-1913.
2. Yap ZY, Park YH, Wortmann SB, et al. Functional interpretation of ATAD3A variants in neuro-mitochondrial phenotypes. *Genome Med*. 2021;13:55.
3. Peralta S, Goffart S, Williams SL, et al. ATAD3 controls mitochondrial cristae structure in mouse muscle, influencing mtDNA replication and cholesterol levels. *J Cell Sci*. 2018;131:jcs217075.
4. Arguello T, Peralta S, Antonicka H, et al. ATAD3A has a scaffolding role regulating mitochondria inner membrane structure and protein assembly. *Cell Rep*. 2021;37:110139.

5. Desai R, Frazier AE, Durigon R, et al. ATAD3 gene cluster deletions cause cerebellar dysfunction associated with altered mitochondrial DNA and cholesterol metabolism. *Brain*. 2017; 140:1595-1610.
6. Gunning AC, Strucinska K, Muñoz Oreja M, et al. Recurrent de novo NAHR reciprocal duplications in the ATAD3 gene cluster cause a neurogenetic trait with perturbed cholesterol and mitochondrial metabolism. *Am J Hum Genet*. 2020;106: 272-279.
7. Vanier MT. Complex lipid trafficking in Niemann-Pick disease type C. *J Inherit Metab Dis*. 2015;38:187-199.
8. Skopkova M, Stufkova H, Rambani V, et al. ATAD3A-related pontocerebellar hypoplasia: New patients and insights into phenotypic variability. *Orphanet J Rare Dis*. 2023;18:92.